Disappearance of Large-scale Field-aligned Current Systems: Implications for the Solar Wind–Magnetosphere Coupling

S. Ohtani

The Johns Hopkins University Applied Physics Laboratory, Laurel, Maryland, U.S.A.

T. Higuchi

The Institute of Statistical Mathematics, Tokyo, Japan

T. Sotirelis and P. T. Newell

The Johns Hopkins University Applied Physics Laboratory, Laurel, Maryland, U.S.A.

Large-scale field-aligned current (FAC) systems occasionally disappear in the midday sector ($9 < MLT < 13$), even though this is the local time sector where FACs tend to be most intense. The present study investigates 26 such events observed by the DMSP-F7 satellite. It is found that the events tend to occur in the winter hemisphere in a certain UT range when the dipole axis was inclined most antisunward and therefore the contribution of solar illumination to the ionospheric conductivity is minimum. Before most events, IMF B_Z was positive, and the solar wind bulk flow momentum was below the average. Although one might expect to see such events when the sign of B_X was unfavorable for merging at the high-latitude tail magnetopause in the winter hemisphere, no clear preference for IMF B_X was found. It was also found that the asymmetry of the ionospheric conductivity between the summer and winter hemispheres suppresses the IMF-dependent characteristics of particle precipitation in the polar cap. These results suggest that ionospheric conductivity not only determines the intensity of FACs for the convection electric field imposed by the solar wind–magnetosphere interaction, but also affects how the magnetosphere interacts with the solar wind.

1. INTRODUCTION

Dayside large-scale field-aligned currents (FACs) are classified into three systems, that is, region 2 (R2), region 1 (R1), and region 0 (R0) systems from equatorward to poleward [*Iijima and Potemra*, 1976]. Good correlation between the intensity of R1 and R0 currents and solar wind parameters [*Iijima and Potemra*, 1982] strongly suggests that these two current systems are generated by interaction between the solar wind and the magnetosphere. The ionospheric distribution of R1 and R0 FACs depends on the IMF orientation, and these FACs are collocated with precipitation of magnetosheath particles (see review article by *Potemra* [1994]). There is little doubt that features related

Magnetospheric Current Systems
Geophysical Monograph 118

to these current systems can be used for a diagnosis of the solar wind–magnetosphere (SW–MS) interaction.

The ionospheric condition is another important factor for the formation of FAC systems, which is demonstrated by strong dependence of the intensity of R1 FACs on the solar zenith angle [*Fujii and Iijima*, 1987]. This dependence suggests that the generation mechanism of FACs is a voltage source, and therefore the current intensity is proportional to ionospheric conductivity. Although this idea is perhaps correct in the first approximation, it is based on the (implicit) assumption that the generation mechanism itself is not affected by the ionospheric condition. The question of whether or not this is truly the case has rarely been addressed observationally.

The issue can be addressed using the following simple considerations. The electric field **E** imposed to the polar cap by the SW–MS interaction should depend on $-\mathbf{v} \times \mathbf{B}$ where **v** and **B** are the magnetosheath flow velocity and the magnetic field in the interaction region. Energy transfer from the solar wind to the magnetosphere is accomplished through the deceleration of the magnetosheath flow, which is attributed to the Lorentz force, $\mathbf{J} \times \mathbf{B}$; **J** is the current density in the interaction region. Thus, we infer that **E** depends on **J**, which is then controlled by ionospheric conductivity σ, provided that the relevant FAC is closed in the interaction region. If this is the case, the role of ionospheric conductivity is more than a parameter that determines the intensity of FACs for given **E**. Is there any observation that can test this idea?

In a separate study [*Higuchi and Ohtani*, 1999] we developed an automatic procedure to identify spatial structures of FACs from satellite magnetometer data and applied it to the entire set of the DMSP-F7 magnetometer data. An unexpected result of that study was that the satellite occasionally observed no large-scale FAC signature in the midday sector. As is shown later, the occurrence of such extraordinary events strongly depends on ionospheric conductivity. By comparing particle and magnetic field signatures between the winter and summer hemispheres and examining solar wind conditions, the present study addresses the role of the ionosphere in the SW–MS interaction.

2. DATA ANALYSIS

We used 1-s magnetometer and particle precipitation data from the DMSP-F7 satellite. DMSP-F7 is a Sun-synchronous satellite with a nearly circular polar orbit at about 835 km altitude, with its ascending and descending nodes at 1030 and 2230 local time (LT), respectively. The orbital period is about 101 min.

We applied the procedure to identify FAC structures [*Higuchi and Ohtani*, 1999] to the entire set of DMSP-F7 magnetometer data acquired from December 1983 to January 1988 (1339 days). The procedure fits line segments to magnetic variations and recognizes a line segment as a FAC sheet if its amplitude is more than 50 nT (47 mA/m if projected to 110 km in altitude). No FAC was detected for 7,956 dayside orbits. It is possible, however, that for skimming orbits, the satellite did not reach a latitude high enough to detect large-scale FACs. Based on orbits for which large-scale FAC systems were detected, we examined the locations of the equatorward-most points of large-scale FACs in the range $09 < \mathrm{MLT} < 13$ and determined the latitude of the 95 percentile from equatorward as a function of MLT. For most of the remaining 5 percent of events, we found that the boundary was misidentified due to apparent artificial signals. As a result, the magnetic latitude of the 95-percentile point is higher than 75° at MLT = 9 and is as high as 79° at MLT = 12. Orbits that did not reach that latitude were removed from the present analysis.

Focusing on 185 events for which the IMP-8 satellite measured the solar wind at $x > +10\ R_E$ and $\sqrt{(y^2 + z^2)} < 30\ R_E$, we visually examined a plot of the east–west magnetic component. If there was a signature that could be associated with large-scale FACs (e.g., a triangle-shaped variation), however small the amplitude, we excluded such an orbit. The final event list contains 26 events.

One may suspect that the satellite did not observe any large-scale FAC signature in these events because the satellite trajectory happened to thread through the demarcation between prenoon and postnoon FAC systems. However, we found consistent dependence of the event occurrence on the dipole tilt angle, which excludes such possibility. Four out of these 26 events occurred in the northern hemisphere between November and January. The remaining 22 events were observed in the southern hemisphere and were also concentrated in winter months: 20 events during May to August and one event in each of March and April. Furthermore, 16 (2) out of 22 (4) events in the southern (northern) hemisphere took place at 12–15 (07–08) UT, when the dipole axis was further inclined antisunward in the corresponding hemisphere. The geographic latitude and longitude of the southern and northern magnetic poles are (–74.2°, 126.1°) and (81.0°, –81.7°), respectively, in PACE coordinates based on the IGRF 85 model (Wing, private communication, 1999). Considering that the southern magnetic pole is more offset from the geographic pole than the northern magnetic pole, the preference of the event occurrence for the southern hemisphere can also be explained in terms of the dipole tilt. We conclude that ionospheric conductivity was extremely asymmetric between the northern and southern hemispheres when the events took place.

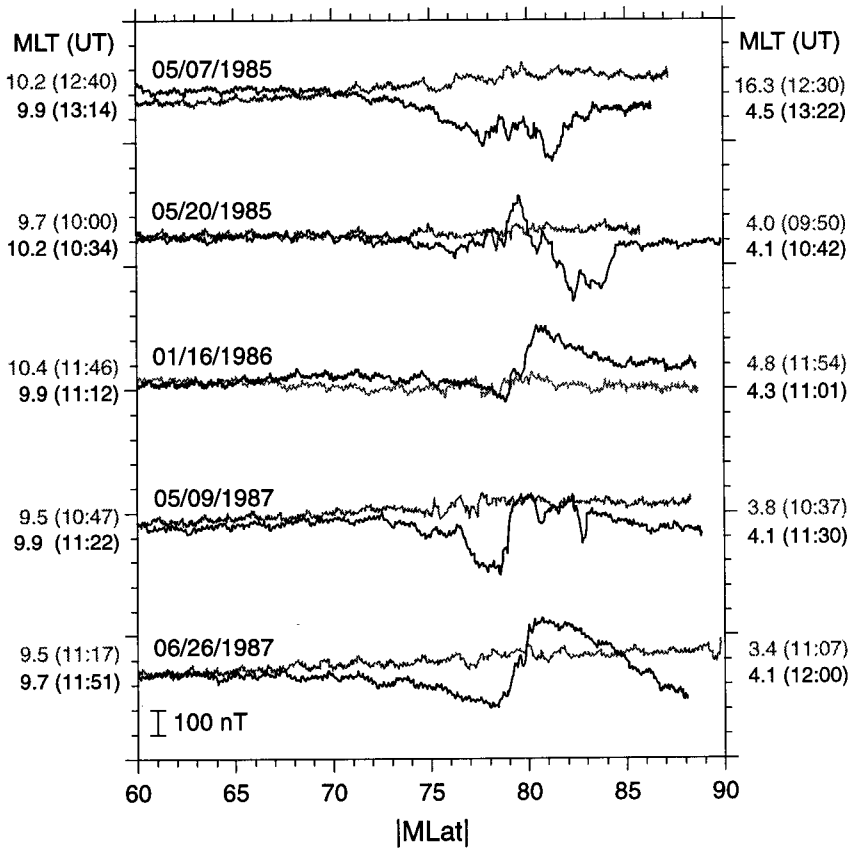

Figure 1. The azimuthal magnetic field component plotted against magnetic latitude for the winter (gray lines) and summer (black lines) hemispheres for five representative events.

Figure 1 plots the azimuthal magnetic field (cross-track) component, B_Z, (positive eastward) against |MLat|, the absolute value of magnetic latitude, for five examples. The gray lines represent data from the winter hemisphere, whereas the black lines represent data from the closest pass of the summer hemisphere. Superposed high-frequency variations and quasi-periodic undulations are common with the DMSP-F7 magnetometer data and are presumably related to the satellite operation; the instrument is mounted on the satellite body. However, the amplitude of these artificial signals is a few tens of nanotesla at most, smaller than the typical amplitude of large-scale FAC signatures by an order of magnitude.

No large-scale magnetic variation can be seen for the winter passes. In contrast, for the summer hemisphere, a three-sheet structure is clear for the events of May 20, 1985; January 16, 1986; and June 26, 1987; and at least two large-scale FAC sheets can be identified for the events of May 7, 1985, and May 9, 1987. The present result interestingly suggests that the intensity of region 2 currents is also strongly controlled by the ionospheric condition like other FAC systems, although it is not a common idea that the region 2 system is driven by a voltage source.

Because the occurrence of events is rather rare, it is expected that there are some external conditions for the disappearance of large-scale FACs. Figure 2 examines the IMF orientation and the solar wind bulk flow momentum nV measured by IMP 8 before the events. Both solar wind plasma and IMF data were averaged over 30 min before the events, and the travel time from the satellite position to the subsolar point was taken into account. Solar wind plasma data were not available for four events, for which the values of B_Z are plotted on the vertical axis. All IMF components are given in GSM coordinates, and in Figure 2b both vertical and horizontal scales are reversed for the events that were observed in the northern hemisphere (NH), which are represented by the open circles.

Three points are clear. First, the distribution of B_Z is biased positively; there are no events with $B_Z < -1$ nT. Second, the values of nV are distributed mostly below its median (the vertical line in Figure 2a). Finally, there is no clear preference for the IMF sector structure, that is, the

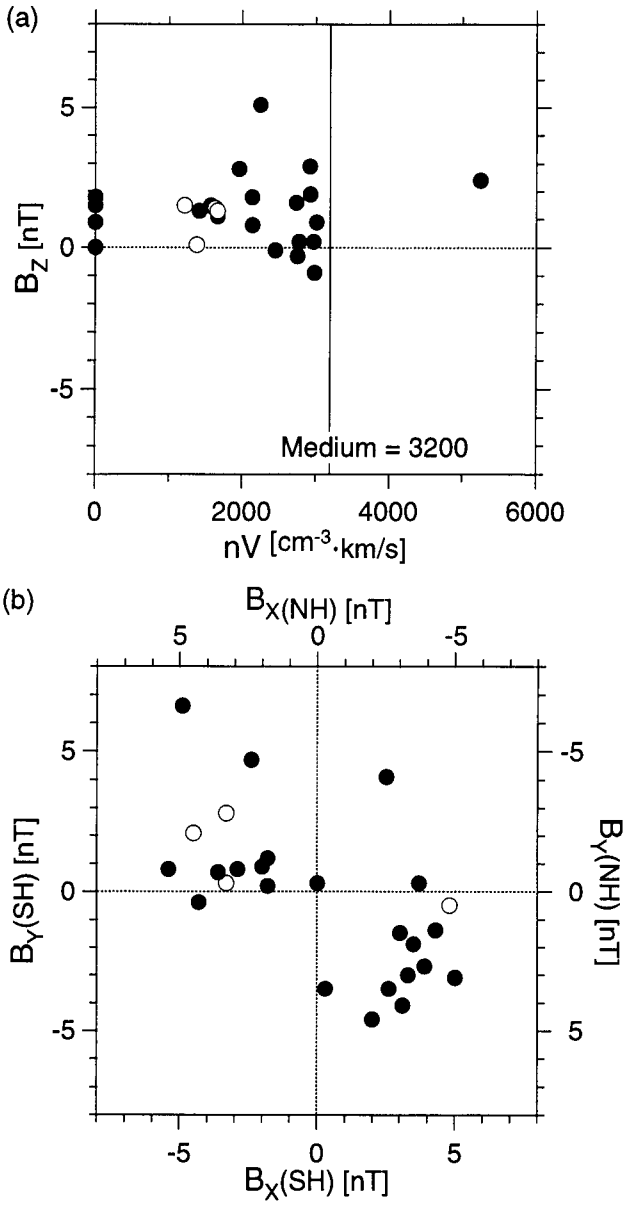

Figure 2. (a) IMF B_Z vs. nV and (b) IMF B_Y vs. B_X before events. For events observed in the northern hemisphere (NH, open circles) both vertical and horizontal scales are inverted in Figure 2b.

sign of IMF B_X or B_Y. The first and second points are important not only because these tendencies are favorable for weak FACs [*Iijima and Potemra*, 1982] but also because under such conditions, the dayside cusp tends to be at higher magnetic latitudes, which is favorable for lower ionospheric conductivity.

The hypothesis of the antiparallel merging predicts that when the IMF is northward, the merging between the IMF and magnetospheric field lines takes place at the tail magnetopause antisunward of the dayside cusp [*Maezawa*, 1976; *Crooker*, 1979], where magnetospheric field lines are open to the solar wind even before merging with the IMF. In fact, the ionospheric distribution of FACs is well explained in terms of this hypothesis [*Potemra et al.*, 1984; *Burch et al.*, 1985; *Cowley et al.*, 1991]. Therefore, the associated FAC is inferred to have separate sources in the winter and summer hemispheres. In contrast, for southward IMF B_Z, the current circuit driven by the SW–MS coupling may be envisioned as a single source at the dayside magnetopause wired to two resistivities in the winter and summer ionospheres. For such a circuit, it would be more difficult to examine the ionospheric feedback to the source mechanism.

When IMF B_Z is positive, positive IMF B_X is more favorable for merging in the southern hemisphere than for merging in the northern hemisphere, and vice versa for negative IMF B_X. Thus it is expected that the events tend to take place when IMF B_X is negative and positive for the southern and northern hemispheres, respectively. The fact that there is no clear preference for the IMF sector structure suggests that the ionospheric condition is the dominant factor for the occurrence of events and the IMF orientation plays, if at all, a secondary role.

Let us examine the winter–summer asymmetry in terms of particle precipitation. An event selected for this purpose took place on January 16, 1986, one of the five events shown in Figure 1. The northern hemisphere was in winter for this event. Figure 3 plots the IMF data acquired by IMP-8 at (25–27, 16–17, 15) R_E for 0900–1200 UT. Although fluctuations are noticeable for each component, the IMF continued to point approximately in the negative X direction throughout the interval. For this orientation, the tail magnetopause in the northern, therefore winter, hemisphere is the preferable site for the merging.

Plate 1a shows two DMSP-F7 trajectories, one in the southern summer (S) hemisphere and the other in the northern winter (N) hemisphere, along with a DMSP-F6 trajectory in the northern winter hemisphere for this event. Plate 1c–1d show the DMSP-F7 measurements of the east–west magnetic component (top panel) and particle precipitation (color-coded panels) in the southern and northern dayside high-latitude regions, respectively. Note that the satellite orbited from poleward to equatorward in the southern hemisphere and vice versa in the northern hemisphere. No noticeable large-scale magnetic variation was observed in the winter hemisphere, whereas three large-scale FAC systems were observed in the summer hemisphere, which are presumably R2, R1, and R0 currents.

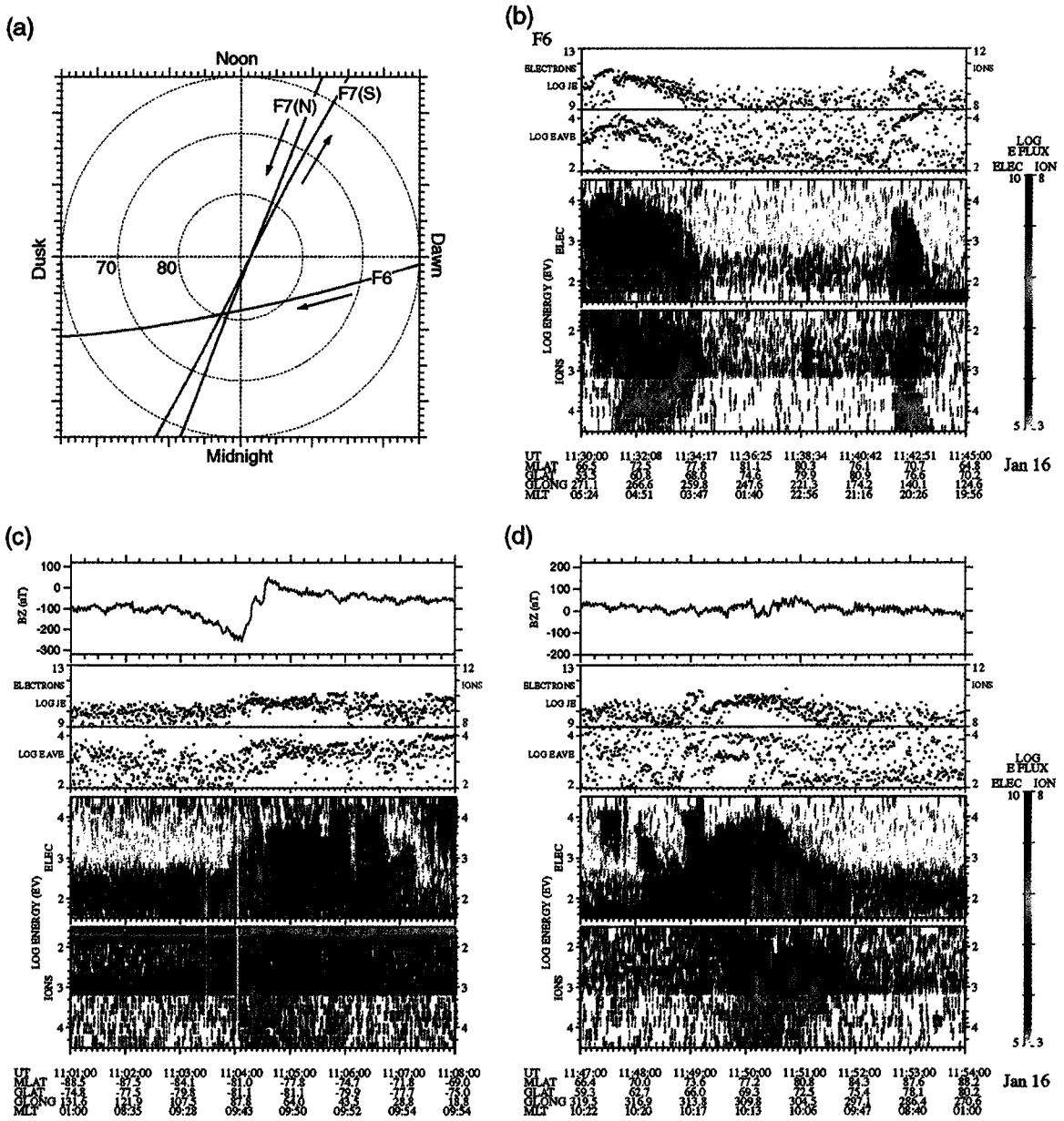

Plate 1. (a) DMSP-F6 and –F7 trajectories in the polar diagram, (b) DMSP-F6 particle precipitation data in the northern (winter) hemisphere, DMSPS-F7 azimuthal magnetic component (B_Z) and particle precipitation data in the (c) southern (summer) and (d) northern (winter) hemisphere. Shown for DMSP particle measurements are energy fluxes, J_E (eV/cm^2 s sr) and the average energies E AVE (eV) for ions (red) and electron (black), and electron and ion differential energy fluxes (eV/cm^2 s sr eV). The energy scale is inverted for the ion E–t diagram.

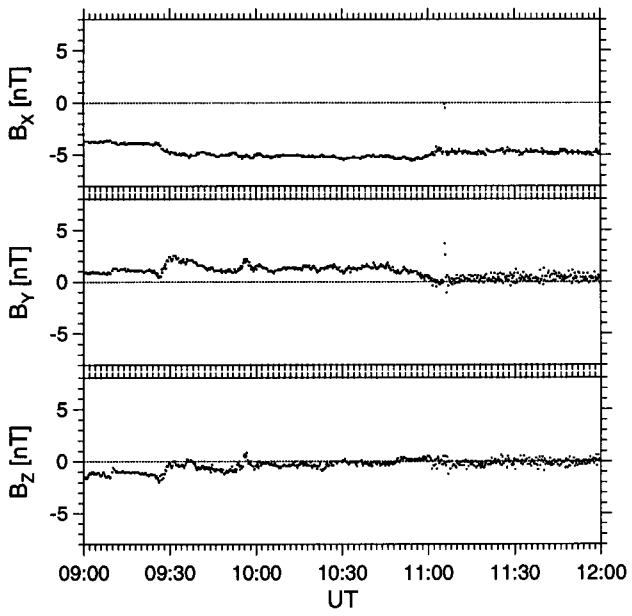

Figure 3. Three IMF components in GSM meassured by IMP 8 at (25–27, 16–17, 15) R_E for the January 16, 1986, event.

At first glance, precipitation signatures look similar between the summer and winter hemispheres. However, there is a noticeable difference in features at the poleward boundary. In the winter (Plate 1d) hemisphere, the termination of low-energy (<1 keV) ion and electron precipitation was coincident. In contrast, in the summer (Plate 1c) hemisphere, bursty electron precipitation extended farther poleward of the termination of ion precipitation. The previous study [*Veselovsky et al.*, 1995] shows that such bursty electron precipitation is better described by the total flux enhancement than by field-aligned acceleration that can be attributed to the magnetosphere–ionosphere coupling; though, this may depend on flux intensity [Figure 7 of *Shinohara and Kokubun,* 1996]. It was also reported that the IMF dependence and other statistical characteristics of such bursty electron precipitation not accompanied by ion precipitation are well explained in terms of the merging process at the high-latitude tail magnetopause [*Shinohara and Kokubun*, 1996]. However, the observed asymmetry is just opposite to what is expected from negative IMF B_X.

Plate 1b shows particle precipitation data from DMSP-F6, which crossed the northern (winter) polar cap during an interval between the summer and winter DMSP-F7 passes; unfortunately, the satellite only skimmed the dayside oval in the opposite hemisphere. No magnetic field data are available from this satellite. The polar cap is void of precipitation except for the isolated low-energy ion and electron precipitation observed around 1139 UT, although this is the hemisphere favorable for observing polar rain for negative IMF B_X [*Fairfield and Scudder*, 1985].

DMSP-F7 particle data were available for 20 out of the 26 events, and we visually examined the E–t diagram for both winter and summer orbits for each event. It is sometimes difficult to uniquely determine the poleward boundary of precipitation. Nevertheless the coincident termination of ion and electron precipitation similar to or even sharper than the January 16, 1986, event, was observed for six other events. All of them took place in the southern winter hemisphere. For three out of the six events, IMF B_X was positive, which is favorable for the merging in the southern winter hemisphere. For those three events, the satellite observed in the northern summer hemisphere, not in the southern winter hemisphere, bursty electron precipitation to extend farther poleward of the termination of ion precipitation. That is, the winter–summer asymmetry was just opposite to what is expected from the sign of IMF B_X, as was the case for the January 16, 1986, event. IMF B_X was negative for another event and was not clear for the other two events. The result suggests that the ionospheric conductivity controls particle precipitation in the open field line region, possibly overturning the preference expected from the IMF orientation. We also found that the energy flux associated with bursty electron precipitation tends to be higher in the summer hemisphere than in the winter hemisphere (not shown).

3. DISCUSSION AND SUMMARY

The present study examined 26 events in which no large-scale FAC signature was observed by DMSP-F7 in the dayside high-latitude region. The events took place in the winter hemisphere in the UT range when the dipole axis was inclined most antisunward and therefore the ionospheric conductivity due to solar illumination was extremely low. In contrast, large-scale FAC systems were clearly observed in the summer hemisphere. The events provide the most ideal opportunity to address the role of the ionosphere in the SW–MS interaction from a winter–summer comparison.

Most of events took place when IMF B_Z was positive and the solar wind bulk momentum was below the average, suggesting that the energy and momentum transfer from the solar wind to the magnetosphere was small. For northward IMF B_Z, it is inferred that field line merging takes place at the tail magnetopause tailward of the dayside cusp, which allows us to assume separate sources of FACs for different hemispheres. Although it is expected that large-scale FACs disappear when the IMF orientation is not favorable for the merging in that hemisphere, no clear preference for the sign

of IMF B_X was found for the event occurrence, indicating that the low ionospheric conductivity is the dominant control factor.

No clear preference for the IMF orientation was found for particle precipitation, either. Instead, the most clear tendency for the examined events is that the bursty electron precipitation in the polar cap is observed farther poleward and with higher energy fluxes in the summer hemisphere than in the winter hemisphere. The result suggests that the ionospheric conductivity is the dominant factor and the preference for the IMF orientation, which is generally the most important parameter for the merging, appears to be suppressed by the extraordinary interhemispheric asymmetry of the ionospheric conductivity.

The role that the ionosphere plays in the magnetospheric electrodynamics may have been underestimated. The results of the present study suggest that the ionospheric conductivity even affects the way the magnetosphere interacts with the solar wind. It is possible, however, that such an active role of the ionosphere is noticeable only when the interhemispheric asymmetry of conductivity is extraordinary and there are separate current sources for different hemispheres, as inferred to be the case for the examined events. Further investigation is required for addressing the mechanism of the ionospheric feedback to the SW–MS interaction.

Acknowledgments. The author (S.O.) thank J. M. Ruohoniemi for fruitful discussions. The DMSP-F7 particle data were provided by C.-I. Meng and D. A. Hardy. The DMSP-F7 magnetometer data were provided by F. J. Rich. The IMP 8 magnetometer data were provided by R. P. Lepping and the National Space Science Data Center through the World Data Center-A for Rockets and Satellites. The IMP 8 solar wind data were provided by the MIT Space Plasma Physics Group. Work at APL was supported by NASA, NSF, and the Office of Naval Research.

REFERENCES

Burch, J. L., P. H. Reiff, J. D. Menietti, R. A. Heelis, W. B. Hanson, S. D. Shawhan, E. G. Shelley, M. Sugiura, D. R. Weimer, and J. D. Winningham, IMF By-dependent plasma flow and Birkeland currents in the dayside magnetosphere, 1, Dynamics Explorer observations, *J. Geophys. Res.*, 90, 1577, 1985.

Cowley, S. W. H., J. P. Morelli, and M. Lockwood, Dependence of convective flows and particle precipitation in the high-latitude dayside ionosphere on the X and Y components of the interplanetary magnetic field, *J. Geophys. Res.*, 96, 5557, 1991.

Crooker, N. U., Dayside merging and cusp geometry, *J. Geophys. Res.*, 84, 951, 1979.

Fairfield, D. H., and J. D. Scudder, Polar rain: Solar coronal electrons in the Earth's magnetosphere, *J. Geophys. Res.*, *90*, 4055, 1985.

Fujii, R., and T. Iijima, Control of the ionospheric conductivities on large-scale Birkeland current intensities under geomagnetic quiet conditions, *J. Geophys. Res.*, *92*, 4505, 1987.

Higuchi, T., and S. Ohtani, Automatic identification of large-scale field-aligned current structures and its application to night-side current systems, this volume, 1999.

Iijima, T., and T. A. Potemra, Field-aligned currents in the dayside cusp observed by Triad, *J. Geophys. Res.*, *81*, 5971, 1976.

Iijima, T., and T. A. Potemra, The relationship between interplanetary quantities and Birkeland current densities, *Geophys. Res. Lett.*, *9*, 442, 1982.

Maezawa, K., Magnetospheric convection induced by the positive and negative z components of the interplanetary magnetic field: Quantitative analysis using polar cap magnetic records, *J. Geophys. Res.*, 81, 2289, 1976.

Potemra, T. A., Sources of large-scale Birkeland currents, in *Physical Signatures of Magnetospheric Boundary Layer Processes*, ed. by J. A. Holtet and A. Egeland, pp. 3–27, Kluwer Academic Publishers, Netherlands, 1994.

Potemra, T. A., L. J. Zanetti, P. F. Bythrow, A. T. Y. Lui, and T. Iijima, B_Y-dependent convection patterns during northward interplanetary magnetic field, *J. Geophys. Res.*, *89*, 9753, 1984.

Shinohara, I., and S. Kokubun, Statistical properties of particle precipitation in the polar cap during intervals of northward interplanetary magnetic field, *J. Geophys. Res.*, 101, *69*, 1996.

Veselovsky, I. S., P. T. Newell, and A. T. Y. Lui, Pervasive small-scale enhancements in mantle and polar rain precipitation, *Geophys. Res. Lett.*, *22*, 3263, 1995.

T. Higuchi, The Institute of Statistical Mathematics, Tokyo 106, Japan.

P. T. Newell, S. Ohtani, and T. Sotirelis, The Johns Hopkins University Applied Physics Laboratory, 11100 Johns Hopkins Rd., Laurel, MD 20723-6099.